Feature Extraction for Oil Spill Detection Based on SAR Images

Camilla Brekke[1,2] and Anne H.S. Solberg[2]

[1] Norwegian Defence Research Establishment,
PO Box 25, NO-2027 Kjeller, Norway
[2] Department of Informatics, University of Oslo,
PO Box 1080 Blindern, 0316 Oslo, Norway

Abstract. Algorithms based on SAR images for the purpose of detecting illegal oil spill pollution in the marine environment are studied. This paper focus on the feature extraction step, aiming at identifying features that lead to significant improvements in classification performance compared to earlier reported results. Both traditional region descriptors, features tailored to oil spill detection and techniques originally associated with other applications are evaluated. Experimental results show an increase from 89% to 97% in the number of suspected oil spills detected.

1 Introduction

Spaceborne Synthetic Aperture Radar (SAR) has proven to be the most efficient satellite sensor for oil spill monitoring of the worlds oceans. Oil spills correlate very well with the major shipping routes, and do often appear in connection to offshore installations. When taking into account how frequent illegal discharges appear, controlled regular oil spills can be a much greater threat to the marine environment and the ecosystem than larger oil spill accidents like the Prestige tanker accident in 2002. Oil spills appear as dark areas in SAR images because oil dampens the capillary waves on the sea surface. A part of the oil spill detection problem is to distinguish oil slicks from other natural phenomena (*look-alikes*) that dampen the short waves and create dark patches in a similar way. Oil slicks may include all oil related surface films caused by oil spills from oilrigs, leaking pipelines, passing vessels as well as bottom seepages, while look-alikes do include natural films/slicks, grease ice, threshold wind speed areas (wind speed $<$ 3 m/s), wind sheltering by land, rain cells, shear zones, internal waves, etc. (see Fig. 1). These ambiguities put a challenge on the selection of suitable features. Research in the field of automatic processing of SAR images in order to detect illegal oil pollution has been ongoing for more than a decade. Several papers, describing fully automatic or semi automatic systems, have been published, e.g. [1, 2, 3]. Little attention seems to have been given the feature extraction step, where parameters used to discriminate oil spills from other phenomena on the sea surface are extracted. An early study on feature extraction based on ERS

H. Kalviainen et al. (Eds.): SCIA 2005, LNCS 3540, pp. 75–84, 2005.

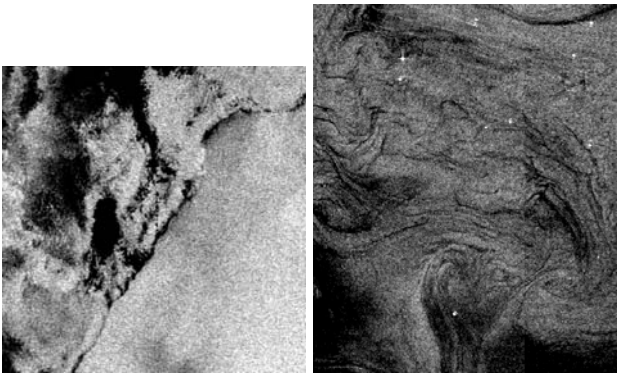

Fig. 1. Look-alikes that occur frequently in low wind areas. ©ESA/KSAT 2003

images is described by Solberg et al. [4], and an evaluation of the discrimination efficiency of typically used features can be found in Topouzelis et al. [5].

Segmentation of dark spots and feature extraction are a crucial part of algorithms for oil spill detection. If a slick is not detected during segmentation, it cannot be classified correctly. If the features have good discriminatory power, the classification problem will be easier and several classifiers can work. We hereby present results from a study aiming at identifying suitable features that lead to significant improvements in classification performance for ENVISAT ASAR Wide Swath Mode (WSM) images. Section 2 describes the automatic algorithm that constitutes the fundament of our work. Section 3 outlines the experiment design and presents the results. Finally, the conclusion can be found in Sect. 4.

2 The Automatic Oil Spill Detection Algorithm

The framework of this study is a fully automatic advanced oil spill detection algorithm developed by Norwegian Computing Center (NR) and University of Oslo. It was originally intended to process ERS-1/-2 SAR images, but it has been extended to work for RADARSAT-1 and ENVISAT. The algorithm includes sensor specific modules for dark spot detection, feature extraction and a classifier discriminating between oil spills and look-alikes (see Fig. 2). Pre-processing, consisting of converting a land mask to the image grid (to avoid re-sampling the speckle pattern) and a normalization of the backscatter with respect to incidence angles, is performed ahead of segmentation for ENVISAT images.

2.1 Dark Spot Detection

The dark spot detector applies adaptive thresholding where the threshold is set k dB below the local mean backscatter level in a large window [3, 6]. The goal is to segment out all possible oil spills. A high number of look-alikes will also be segmented out, but these will hopefully be classified as look-alikes during

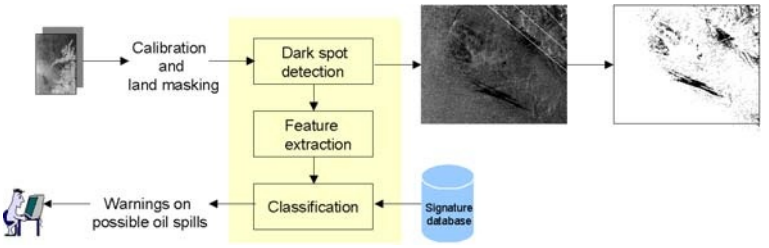

Fig. 2. The oil spill detection algorithm and its context. Arrows indicate data flow

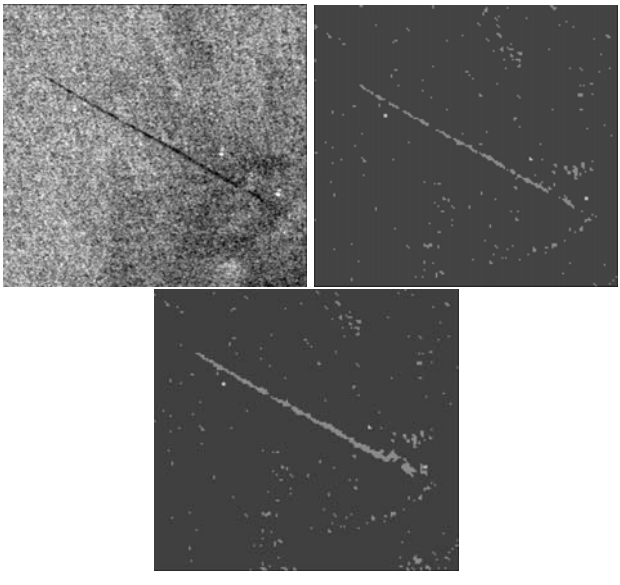

Fig. 3. Section of an ENVISAT ASAR WSM image (19 September 2003), original segmented image and the improved result

classification. The thresholding is done in a two level pyramid after applying a simple speckle filter with a small window. k is determined based on the wind level. If no wind information is available, we use the power-to-mean (PMR) ratio of the local surroundings as an indication of the number of look-alikes in the scene. The number of observed look-alikes will vary according to local wind conditions. Thin linear slicks have a tendency to be fragmented in the segmentation process. An approach, searching for additional slick pixels in an extended object-oriented bounding box surrounding the slick, has been developed. Only pixels close to an edge are accepted and merged with the original segmented image (see Fig. 3).

2.2 Slick Feature Extraction

After segmentation, a set of features are computed and extracted from every region above a certain minimum size.

Existing Set of Features. A basic set of features was described in [3]. Due to page limits, these are not described in detail here. The features are a mix of standard region descriptors and features tailored to oil spill detection (see Table 1). Not all of these features were found to be robust and yield the best

Table 1. Basic feature vector components

#	Feature	Description
1	WIND	The wind level in the scene.
2	MOM (Moment)	1st planar moment of the region.
3	COMPL (Slick complexity)	$C = P^2/A$, P is the perimeter and A is the area of the region.
4	PMR (Power-to-mean ratio)	Homogeneity of the surroundings. Defined as σ_b/μ_b. σ_b and μ_b are the standard deviation and mean of near-by background pixels.
5	LCONT (Local contrast)	Defined as $\mu_b - \mu_r$, μ_b is the background pixel mean and μ_r is the region pixel mean.
6	THICK (Thickness)	Thickness of the region, defined as the ratio between the area of the region and the diameter of the region skeleton.
7	NOFSN (Number of small neighbours)	The number of small neighbouring regions.
8	BGRAD (Border gradient)	The mean of the magnitude of the region border gradient. Sobel is used to compute the gradients.
9	SMC (Smoothness contrast)	Defined as the ratio between the ratio of the number of region pixels and the sum of the region gradient values, and the ratio of the number of background pixels and the sum of the background gradient values.
10	AREA	The number of pixels in the region.
11	DIST (Distance)	The distance from the region to closest bright spot (ship).
12	NLN (Number of large neighbours)	The number of large neighbouring regions.
13	NREG (Number of regions)	The total number of detected regions in the scene.

description of the type of information it was meant to extract. The goal of this paper is to find new features and compare their performance to the existing.

New Features. The basic feature set has been extended with the features described in the following.

Slick Border Gradient. The Sobel operator is an edge detector that has been suggested used for oil spill border gradient estimation, see e.g. [7, 3]. Originally, the mean value of the magnitude was applied in the BGRAD feature in our system (see Table 1). It works generally well, but it seems to give inaccurate

results for thin linear regions. The main problem is that the edge response does not match the real borders of the region. The top row to the right of Fig. 4 illustrates the response of the Sobel operator on the oil spill to the left in the same figure. The largest gradient magnitude appears outside the true region border. The following 4 additional convolution masks are suggested for gradient estimation of thin oil spill regions:

$$\begin{bmatrix} 0&0&0&0&0\\ 0&0&0&0&0\\ 1&1&-4&1&1\\ 0&0&0&0&0\\ 0&0&0&0&0 \end{bmatrix}, \begin{bmatrix} 0&0&1&0&0\\ 0&0&1&0&0\\ 0&0&-4&0&0\\ 0&0&1&0&0\\ 0&0&1&0&0 \end{bmatrix}, \begin{bmatrix} 0&0&0&0&1\\ 0&0&0&1&0\\ 0&0&-4&0&0\\ 0&1&0&0&0\\ 1&0&0&0&0 \end{bmatrix} and \begin{bmatrix} 1&0&0&0&0\\ 0&1&0&0&0\\ 0&0&-4&0&0\\ 0&0&0&1&0\\ 0&0&0&0&1 \end{bmatrix}$$

The magnitude of the pixel gradient is found by $\bigtriangledown(p) = max\{\bigtriangledown(p)_i : i = 1\ to\ 4\}$ where p = current pixel, i = mask. The bottom row of Fig. 4 illustrates the response to these masks. If the Sobel operator gives stronger magnitude response to any of the border pixels that value is kept, otherwise the response from the additional masks are used. The mean of this border gradient detector gives us an indication of the contrast to the surrounding background, and is used in the improved feature BGRAD_NEW to replace BGRAD in Tabel 1.

Texture. Texture refers to the properties that represent the surface or structure of an object. There is no precise mathematical definition of texture due to its wide variability. In Table 1 there is no feature representing the texture of the slick it self. The PMR of the slick, defined as σ_r/μ_r where σ_r is the standard deviation and μ_r is the mean value of the slick, has earlier been suggested by Solberg et al. [3]. Frate et al. [1] have simply used the standard deviation of the slick as a texture measure. However, the standard deviation of the intensity values of the

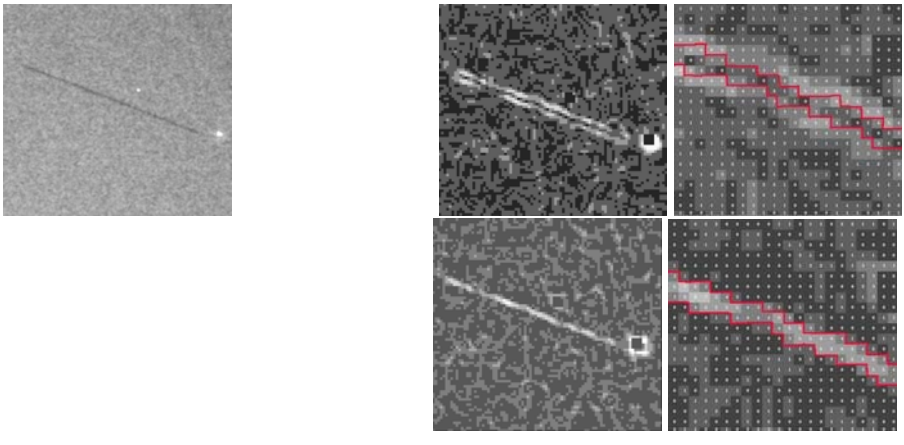

Fig. 4. Left: Section of an ENVISAT ASAR WSM image (24th of July 2003). Top right: Response from the Sobel operator (real region borders indicated by a red line). Bottom right: Response from the improved border gradient estimation

pixels belonging to a slick is highly correlated with the area/size of the region. This is due to the inherent nature of speckle statistics. Speckle is a large problem in SAR images since even a homogeneous area has a statistical distribution with large standard deviation. As the region grows larger the variance in intensity values will increase as well. A better choice would be to look at σ_r^2/A, where σ_r is the standard deviation and A is the area of the slick. After normalization by area, the feature values of larger oil spills are comparable to smaller samples.

Geometrical Complexity. Features, based on the ratio between the perimeter P and the area A, aiming at describing the shape complexity of regions have been used in several algorithms [1, 2, 3, 5]. In [3] the complexity feature is implemented as $C = P^2/A$ (see Table 1) while in [1] it is implemented as $C = P/2\sqrt{\pi A}$[1]. Generally, this feature is expected to get a small numerical value for regions with simple geometry, while a larger value for more complex regions. In contradiction to common intuition, the thin linear oil spill to the right of Fig. 5 gets a larger complexity value than both the others when using the formula in Table 1. Frate et al.'s [1] formula gives very similar but differently scaled results. This indicates that the ratio between perimeter and area is not a good complexity measure as it is not possible to separate complex shaped slicks from linear slicks. This weakness is also pointed out by Nixon and Aguado [8], and Topouzelis et al. [5] found that the feature gave little contribution to oil spill detection. To resolve this ambiguity we could introduce additional shape measures, or replace this measure with a more robust one. A possibility is to look at the number of branching points[2] in the skeleton of each region (see Fig. 6). Because we only look at the number of branching points, the information level is decreased so much that again it is often not possible to distinguish simple regions from more complex ones (e.g. a straight line would get the same feature value as an "S" shaped region). Contour or snake models are commonly applied to ultrasound image segmentation. Lobregt and Viergever [9] define local curvature $\boldsymbol{c}_i$ as the difference between the directions of two edge segments that join at a vertex: $\boldsymbol{c}_i = \hat{d}_i - \hat{d}_{i-1}$ (see Fig. 7). The local curvature has length and direction. This provides a measure of the angle between to joining edge segments. The length of the curvature vector depends only on this angle and is not influenced by the lengths of the two edge segments. In our implementation, we have traced the boundary of every region and inserted vertexes with a three-pixel spacing. The angle between two edge segments is calculated as described above, and the final CURVATURE feature is the sum of all local curvature measures (changes of slope) along the boundary.

2.3 Statistical Classification

After a set of M dark spots has been detected, we want to classify them as either oil spills or look-alikes. A classification algorithm has been developed, combining

[1] This quantity is referred to as *compactness* in [8]. It measures the ratio between the area of the shape and the circle traced with the same perimeter: $C = 4\pi A/P^2$.

[2] *The number of branching points*: a point with three lines or more connected to it.

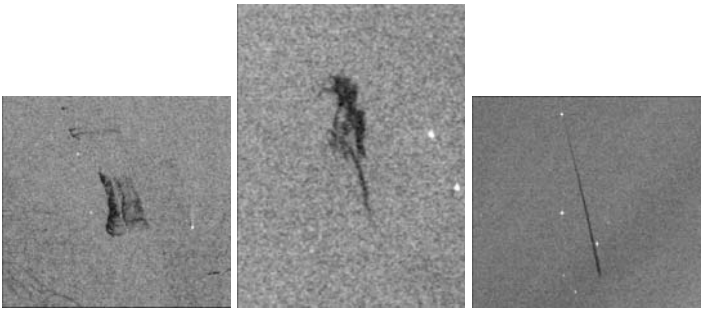

Fig. 5. Sections of ENVISAT ASAR WSM images (8th of March 2003, 7th of August 2003 and 12th of February 2003)

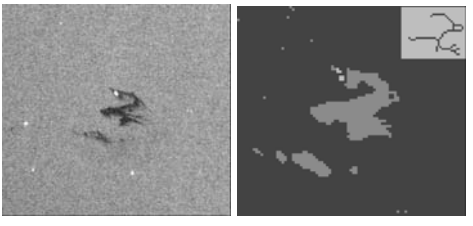

Fig. 6. Section of an ENVISAT ASAR WSM image (3rd of August 2003) with the segmentation result of the oil spill and its skeleton (upper right corner)

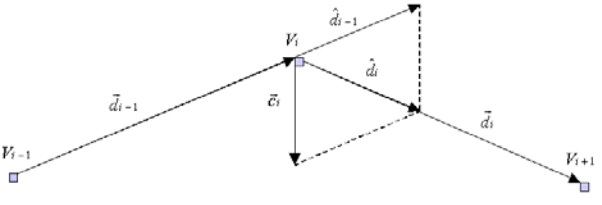

Fig. 7. Local curvature $\boldsymbol{c}_i$. $\hat{d}_{i-1}$ and $\hat{d}_i$ are the directions (unit vectors) of the edge segments $\boldsymbol{d}_{i-1}$ and $\boldsymbol{d}_i$ meeting at vertex V_i

a statistical model for oil spills of different shapes and seen under different wind conditions, a prior model for the probability of observing oil and look-alikes, and a rule-based approach which take care of certain expert knowledge related to oil spill detection [3]. Only the features #3 - #9 from Table 1 are used to compute the probability densities. Feature #1 and #2 are used to group the samples first in two different subclasses based on wind, and then five different subclasses for each wind level according to their value of the shape descriptor. The rest of the features are included in rule-based corrections of the class-conditional densities. The classifier is trained on a large set of labelled samples. Diagonal covariance matrices are used because the number of oil spills in each sub class is small.

3 Performance Testing

3.1 Experimental Design

Our results are based on a large set of 83 ENVISAT ASAR WSM images. We have benchmark results and aircraft verifications collected by the European Commission (EC) project Oceanides for 27 of the scenes. This is done in collaboration with Kongsberg Satellite Services (KSAT), QinetiQ, NR, German (MLZ) and Finnish (SYKE) pollution control authorities [10]. For performance testing, the SAR scenes are split into two parts. 56 of the scenes are used for training and adjusting the model parameters, and the 27 benchmark scenes are used as a validation/test set to estimate the generalization error. The training set is collected from the German and Finnish Baltic Sea, the North Sea and some along the Norwegian coastline during March to December 2003 and January to April 2004. The benchmark set is collected mainly from the German and Finnish Baltic Sea and the German North Sea between July and December 2003.

3.2 Classification Results

Table 2 gives a definition of the new set of features. The results from a forward selection of the features #3 - #13 in Table 1 in addition to the new features in Table 2 are plotted in Fig. 8. As the figure illustrates, adding more and more features gives little added value to the performance results. More research on which combination of features is the most optimal for oil spill detection is needed. The first line of Table 3 presents the results from classifying the complete benchmark set of 27 scenes by applying feature #3 - #9 in Table 1. A doubt category was used to mark slicks we were uncertain about. These cases are left out of the classification results. The classification was done without the rule-based corrections of the class-conditional densities described in Solberg et al. [3]. The rule-based corrections are based on the observed values of the basic

Table 2. Extended set of features

# Feature	Description
14 BGRAD_NEW	The mean border gradient. A combination of Sobel and the four additional masks described in Sect. 2.2 is used as a gradient detector.
15 VAR_AREA_SLICK	Defined as the ratio, σ_r^2/A, of the slick standard deviation σ_r and area A.
16 CURVATURE	Defined as the sum of all local curvature measures along the boundary.

Table 3. Classification results based on the basic set and the new feature vector

Feature set	Correctly classified oil spills	Correctly classified look-alikes
Basic set (#3-#9)	89%	90%
New set (#16, #4-#7, #14, #9, #15)	97%	90%

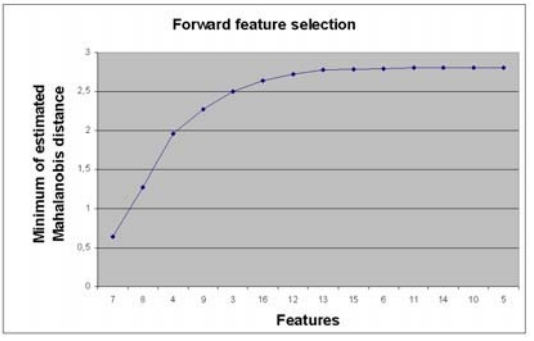

Fig. 8. Forward feature selection according to the minimum estimated Mahalanobis distance. 3: COMPL, 4: PMR, 5: LCONT, 6: THICK, 7: NOF_SMALL_NEIGHB, 8: BGRAD, 9: SMOOTH_CONTR, 10: AREA, 11: DIST, 12: NOF_LARGE_NEIGHB, 13: NOF_REGIONS, 14: BGRAD_NEW, 15: VAR_AREA_SLICK and 16: CURVATURE

set of features on the training set. When replacing some of the features, the rules have to be modified. This is not done in the current analysis, but will be done in the near future. Thus, the rule-based corrections are left out of all performance results hereby presented. The first line of Table 3 can for this reason be used as a reference for the second line. The second line presents the final classification results after substituting the COMPL feature in Table 1 with CURVATURE, BGRAD with the improved border gradient detector BGRAD_NEW, and adding the VAR_AREA_SLICK as an additional feature to the feature vector.

4 Conclusion

Experimental results from an evaluation of features for oil spill detection based on SAR images have been presented. We have studied properties of the border gradient and texture measures of the slicks. In addition, we have compared several features measuring geometrical complexity. The use of curvature, as adopted from the well-known concepts of contour models (snakes), is suggested as a more robust feature than those commonly applied in the oil spill remote sensing literature. The features have been evaluated on a large set of 83 ENVISAT ASAR WSM images, achieving an improvement from 89% to 97% in the number of suspected oil spills classified correctly. Further research should focus on increasing the number of 90% correctly classified look-alikes, i.e. decreasing the false alarm rate. The rule-based corrections left out in this experiment need be to modified according to the new feature set, because the rule-based corrections are important in reducing the number of false alarms. As features extracted vary between methods, our future work will also include a comparison between our final selection of features and other combinations suggested in the literature.

Acknowledgments

The work of Camilla Brekke was funded by Norwegian Research Council and Norwegian Defence Research Establishment. The authors would like to thank Oceanides for the ENVISAT scenes.

References

1. Frate, F.D., Petrocchi, A., Lichtenegger, J., Calabresi, G.: Neural networks for oil spill detection using ERS-SAR data. IEEE Trans. on Geos. and Remote Sensing **38** (2000) 2282–2287
2. Fiscella, B., Giancaspro, A., Nirchio, F., Pavese, P., Trivero, P.: Oil spill detection using marine SAR images. Int. J. of Remote Sensing **21** (2000) 3561–3566
3. Solberg, A.H.S., Storvik, G., Solberg, R., Volden, E.: Automatic detection of oil spills in ERS SAR images. IEEE Trans. on Geos. and Remote Sensing **37** (1999) 1916–1924
4. Solberg, A.H.S., Solberg, R.: A large-scale evaluation of features for automatic detection of oil spills in ERS SAR images. Proc. IGARSS'96, 27-31 May **3** (1996) 1484–1486
5. Topouzelis, K., Karathanassi, V., Pavlakis, P., Rokos, D.: Oil spill detection: SAR multi-scale segmentation & object features evaluation. Proc. SPIE. Remote sensing of the ocean and sea ice 2002, 23-27 Sept. **4880** (2003) 77–87
6. Solberg, A.H.S., Brekke, C., Solberg, R., Husøy, P.O.: Algorithms for oil spill detection in Radarsat and ENVISAT SAR images. Proc. IGARSS'04, 20-24 Sept. **7** (2004) 4909–4912
7. Girard-Ardhuin, F., Mercier, G., Garello, R.: Oil slick detection by SAR imagery: potential and limitation. Proc. OCEANS'03 **1** (2003) 164–169
8. Nixon, M., Aguado, A.: Feature Extraction & Image Processing. Newnes (2002)
9. Lobregt, S., Viergever, M.A.: A discrete dynamic contour model. IEEE Trans. on Med. Imaging **14** (1995) 12–24
10. Indregard, M., Solberg, A., Clayton, P.: D2-report on benchmarking oil spill recognition approaches and best practice. Technical report, Oceanides, EC, Archive No. 04-10225-A-Doc, Contr. No: EVK2-CT-2003-00177 (2004)